Hindawi
Journal of Spectroscopy
Volume 2017, Article ID 5725340, 8 pages
https://doi.org/10.1155/2017/5725340

Research Article

Photo-Induced Cell Damage Analysis for Single- and Multifocus Coherent Anti-Stokes Raman Scattering Microscopy

Takeo Minamikawa,[1,2] Yoshinori Murakami,[2] Naokazu Matsumura,[2] Hirohiko Niioka,[2] Shuichiro Fukushima,[2] Tsutomu Araki,[2] and Mamoru Hashimoto[2,3]

[1]*Graduate School of Technology, Industrial and Social Sciences, Tokushima University, 2-1 Minami-Josanjima, Tokushima 770-8506, Japan*
[2]*Graduate School of Engineering Science, Osaka University, 1-3 Machikaneyama, Toyonaka, Osaka 560-8531, Japan*
[3]*Graduate School of Information Science and Technology, Hokkaido University, Kita 14, Nishi 9, Kita-ku, Sapporo, Hokkaido 060-0814, Japan*

Correspondence should be addressed to Takeo Minamikawa; minamikawa.takeo@tokushima-u.ac.jp

Received 28 April 2017; Revised 18 July 2017; Accepted 8 August 2017; Published 1 October 2017

Academic Editor: Young Jong Lee

In this study, we investigated photo-induced damage to living cells during single- and multifocus excitations for coherent anti-Stokes Raman scattering (CARS) imaging. A near-infrared pulsed laser (709 nm) was used to induce cell damage. We compared the photo-induced cell damage in the single- and the multifocus excitation schemes with the condition to obtain the same CARS signal in the same frame rate. For the evaluation of cell viability, we employed 4′,6-diamidino-2-phenylindole (DAPI) fluorophores that predominantly stained the damaged cells. One- and two-photon fluorescence of DAPI fluorophores were, respectively, excited by an ultraviolet light source and the same near-infrared light source and were monitored to evaluate the cell viability during near-infrared pulsed laser irradiation. We found lower uptake of DAPI fluorophores into HeLa cells during the multifocus excitation compared with the single-focus excitation scheme in both the one- and the two-photon fluorescence examinations. This indicates a reduction of photo-induced cell damage in the multifocus excitation. Our findings suggested that the multifocus excitation scheme is expected to be suitable for CARS microscopy in terms of minimal invasiveness.

1. Introduction

Coherent anti-Stokes Raman scattering (CARS) microscopy and the other coherent Raman scattering microscopy are now promising techniques to three-dimensionally visualize molecular species and structures of biological samples without staining [1–7]. CARS microscopy generally employs two highly synchronized picosecond mode-locked lasers to induce coherent molecular vibrations by adjusting the frequency difference of these excitation lasers (ω_1 and ω_2) at a molecular vibration ($\Omega = \omega_1 - \omega_2$). The CARS signal at the anti-Stokes frequency region ($\omega_{as} = 2\omega_1 - \omega_2$) is generated via a coherent interaction of the one of the excitation light (ω_1) and the coherent molecular vibration. Since the CARS process gives a strong signal compared with spontaneous Raman scattering process, CARS microscopy has been applied for real-time imaging *in vitro* and *in vivo* [8–10].

For further increase of the imaging speed of CARS microscopy, the maximization of excitation laser power is a critical issue. However, photo-induced damage limits the applied laser power for noninvasive real-time imaging of the CARS microscopy. In CARS microscopy employing near-infrared pulse lasers, the photo-induced damage is dominantly caused by multiphoton induced phenomena, such as multiphoton absorption, oxidation stress, and free-radical generation [11–14]. The probability of the multiphoton events increases nonlinearly proportional to the peak intensity of an excitation pulse laser. Regulation of the peak intensity is thus essential for the noninvasive CARS microscopy.

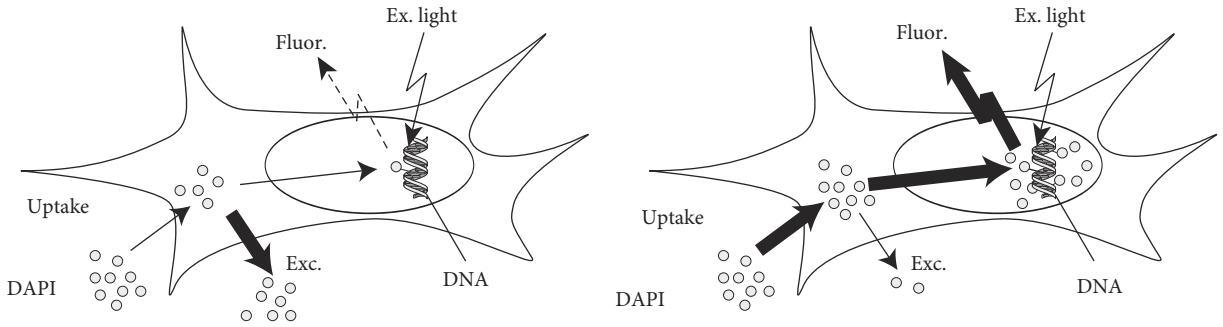

Figure 1: Staining mechanism of DAPI fluorophores in vital and damaged cells. Exc: excretion of DAPI; Fluor: fluorescence of DAPI. The thickness of arrows indicates relative reaction frequency of each event.

To avoid the photo-induced damage, we recently developed a multifocus excitation CARS microscopy [9, 15, 16]. The multifocus excitation method forms multiple focal spots on a sample by using microlens array, and CARS signals generated at the focal spots are simultaneously observed with a two-dimensional image sensor. The total intensity of CARS signal (I_{CARS}) in the multifocus excitation scheme is expressed as follows:

$$I_{\mathrm{CARS}} \propto \int_0^{\tau} \left\{ \chi^{(3)} \right\}^2 {I_1}^2 I_2 N dt, \tag{1}$$

where $\chi^{(3)}$, I_1, I_2, τ, and N are third-order nonlinear susceptibility, the intensity of excitation lasers operating at the optical frequency of ω_1 and ω_2, dwell time and the number of focal spots, respectively. According to (1), it is expected that the multifocus excitation method has a great advantage to prolong image exposure time proportionally to the number of focal spots and realizes high-speed CARS imaging without the increase of the excitation laser power of each focal spot. The efficacy of increasing the focal spots in one- and multiphoton microscopies has been discussed by several researchers [9, 17–23]; however, the photo-induced cell damage in the case of CARS microscopy with the multifocus excitation scheme, which employs near-infrared pulsed laser without any dyes, has not been demonstrated yet except our preliminary work [24].

In the present study, we sought to investigate the photo-induced damage on living cells during single- and multifocus excitations for CARS imaging. To evaluate the photo-induced damage during laser irradiation, we utilized 4′,6-diamidino-2-phenylindole (DAPI) fluorophores. The accumulation of the DAPI fluorophores inside the cells depends on the regulation state of molecular transport across the cell membrane; that is, the fluorophores hardly penetrate to the cell membrane of vital cells, while easily penetrating to that of dead and/or damaged cells. Since DAPI fluorophores specifically bind to the adenine-thymine regions of DNA strands in the nucleus, resulting in an increase in fluorescence intensity, the DAPI fluorescence can be used as an effective indicator for determination of cell viability. According to such advantage of the DAPI fluorophores, we have observed fluorescence of DAPI-stained cells to examine the progression of photo-induced damage that may be caused by irradiation of a near-infrared laser light in CARS microscopy.

2. Materials and Methods

2.1. Photo-Induced Cell Damage Analysis. Photo-induced damage of cells was estimated by using 4′,6-diamidino-2-phenylindole (DAPI) fluorophores. The DAPI fluorophore shows a weak signal in an aqueous solution but exhibits strong fluorescence upon binding to double strand DNA in the nucleus of cells. Since the molecular transport of DAPI fluorophores across the cell membrane is regulated in vital cells, in which the uptake is suppressed and the excretion is enhanced, the vital cells are difficultly stained with DAPI fluorophores. As such, the cellular uptake regulation of the vital cells is beneficial to reduce the initiation of dye-dependent cell damage even when the cells are immersed in the dye solution. When photo-induced cell damage occurs, the molecular transport of DAPI fluorophores is enhanced due to the decrease of membrane functions (Figure 1). Therefore, by observing the fluorescence intensity of DAPI fluorophores, we can evaluate cell viability.

2.2. Optical Setup. The optical setup for the evaluation of photo-induced cell damage is shown in Figure 2. A picosecond mode-locked Ti:sapphire laser (the center wavelength of 709 nm, the pulse duration of 5 ps, and the repetition rate of 80 MHz; Tsunami, Spectra-Physics) was used as a laser source for the cell damage induction. For the single-focus excitation, we used nonresonant/resonant galvano mirror pair scanner (128 lines, 125 frames/s) to scan the focal spot. For the multifocus excitation, we used a microlens array scanner (128 lines, 1000 fps). The laser beams from the optical path of the single- and the multifocus excitations were led to an optical microscope (Ti-U, Nikon) and were irradiated onto a sample via an objective lens (x40, NA 0.85, S Fluor, Nikon). The laser beam of the single- or the multifocus excitation which leads to the sample was switched by changing the mirror orientation at the optical microscope.

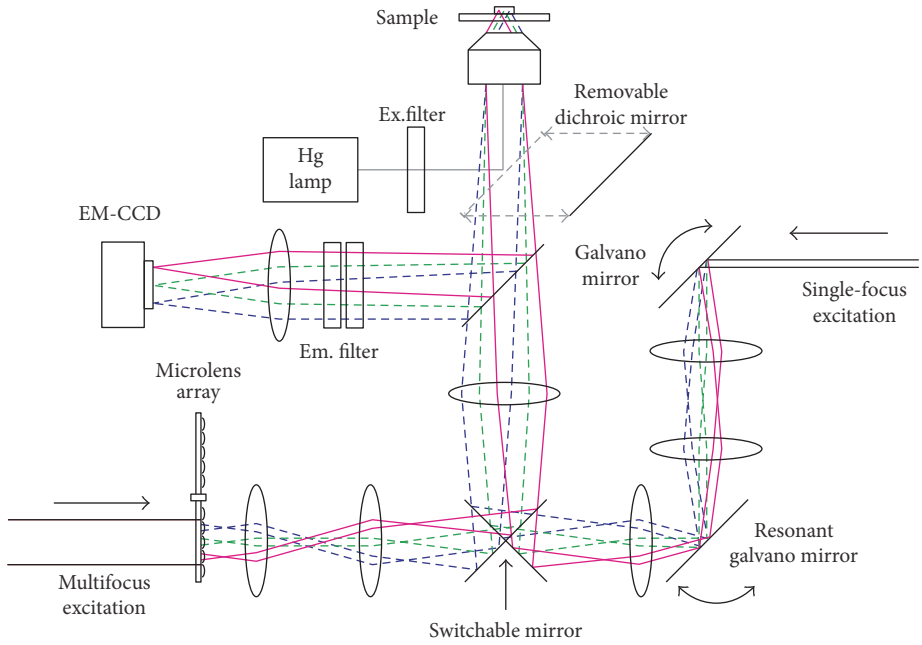

Figure 2: Optical setup of single- and multifocus excitation system for photo-induced damage analysis.

According to (1), the condition to obtain the same CARS signals in single- and multifocus excitations is expressed as follows:

$$I_{s,1}{}^2 I_{s,2} = N I_{m,1}{}^2 I_{m,2}, \tag{2}$$

where I_s, I_m, and N are the excitation laser power of single- and multifocus excitations and the number of focal spots in the multifocus excitation, respectively. The number suffixes of I_s and I_m indicates the two laser sources generally employed in CARS microscopy. In this study, we assumed that the two laser sources were the same laser source with the intensity of I_{ex}.

Fluorescence of DAPI fluorophores at the wavelength of 460 nm with 50 nm bandwidth was observed with an EM-CCD camera (Luca, Andor). For the detection of the one-photon fluorescence signal that is usually analyzed in conventional fluorometry, the 365 nm line of a Hg lamp was additionally prepared as the excitation light source. To avoid the two-photon fluorescence contribution excited by the cell damage induction laser source, we sequentially performed the irradiation of cell damage induction laser and the fluorescence observation. In the two-photon fluorescence detection, the observation of two-photon fluorescence and the damage induction on cells was simultaneously performed using the same laser source.

To clarify the environmental effect of cell damage other than the laser irradiation, we also observed one-photon and two-photon fluorescences of DAPI fluorophores in HeLa cells with a control condition. In the evaluation with one-photon fluorescence, we did not irradiate the cell damage induction laser. In the evaluation with two-photon fluorescence, we employed the single-focus excitation scheme with low excitation laser power of 3.7 mW. Temperature of the sample stage was kept at 37°C to provide a reliable assay.

2.3. Sample Preparation. HeLa cell was used for the photo-induced damage evaluation. The cells were cultured in Dulbecco's modified Eagle's medium with 10% (v/v) fetal bovine serum and 1% (v/v) antibiotic/antimycotic solution. For the photo-induced damage evaluation, HeLa cells were incubated on a glass-bottomed dish at 37°C in 5% CO_2 for 24 h, and then the culture medium was replaced with a pH-indicator-less modified Tyrde's solution (1 mM D-glucose, 145 mM NaCl, 1 mM $MgCl_2{\cdot}6H_2O$, 4 mM KCl, 10 mM HEPES, 1 mM $CaCl_2$, pH 7.4) that was maintained at 37°C with a rubber heater to avoid light absorption and unfavorable autofluorescence by a pH indicator. For the observation of fixed HeLa cells, we used 4% paraformaldehyde diluted in distilled water for the fixation of HeLa cells.

DAPI fluorophore (Sigma-Aldrich, excitation max.: 358 nm, emission max.: 461 nm) of 12.3 mM was prepared as a stock dye solution. The dye solution was dropped into the Tyrode's solution to be the desired concentration just before the measurement. Final concentration of the dye was 71.5 μm in the Tyrode's solution.

3. Results

Firstly, we evaluated the photo-induced cell damage with the two-photon fluorescence scheme. To evaluate the photo-induced cell damage in terms of DAPI fluorescence, we define a normalized two-photon fluorescence value $S_{\text{damage,TPF}}$ as follows:

$$S_{\text{damage,TPF}} = \frac{I_{\text{TPF}}}{N I_{\text{ex}}{}^2}, \tag{3}$$

where I_{TPF}, N, and I_{ex} are the two-photon fluorescence signal observed with an image sensor, the number of focal spots and the excitation laser power, respectively. Figure 3 shows

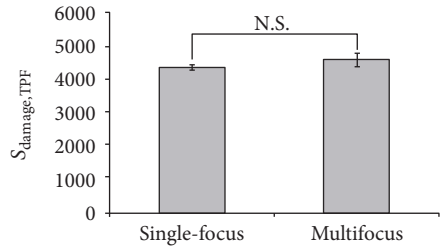

Figure 3: Normalized two-photon fluorescence value $S_{damage,TPF}$ of a fluorescent bead. N.S. indicates not significant.

$S_{damage,TPF}$ values of a fluorescent bead calculated by (3). The excitation laser power of each spot was 27.8 mW for a single-focus excitation and 14.5 mW with 7 focal spots for a multifocus excitation to obtain the same CARS signals as described in Materials and Methods. We obtained equivalent $S_{damage,TPF}$ value with no significant difference in both the single- and the multifocus excitation schemes, indicating $S_{damage,TPF}$ value is usable for the evaluation of photo-induced cell damage.

Temporal behaviors of normalized two-photon fluorescence value $S_{damage,TPF}$ during the laser irradiation onto individual HeLa cells were shown in Figure 4. Laser irradiation and the mixing of the DAPI fluorophores into the culture medium were performed at 0 min. Two-photon fluorescence image was observed continuously with the averaging time of 32 ms/frame. The temporal behaviors of the diffusion of DAPI fluorophores into cell nucleus were measured with a fixed HeLa cell as shown in Figure 4(a). The DAPI fluorophores were well diffused within a few minutes to exhibit the DAPI fluorescence at the nucleus of the fixed HeLa cells.

In the early stage of the laser irradiation within a few minutes, the temporal behaviors of the normalized two-photon fluorescence value $S_{damage,TPF}$ were similar in both the single- and the multifocus excitations owing to the regulation of membrane transport of DAPI molecules of undamaged HeLa cells (Figure 4(a)). In the single-focus excitation, the normalized two-photon fluorescence values of almost half of the HeLa cells significantly increased after 5 to 10 min of the laser irradiation compared with that in the multifocus excitation. It might indicate that the membrane function of the molecular transport regulation of HeLa cells was suppressed due to the strong irradiation of laser light. In contrast, in the multifocus excitation, most of the HeLa cells exhibited the low normalized two-photon fluorescence values that was similar to the behavior of the control condition, indicating the membrane function of the molecular transport regulation of HeLa cells worked even with the laser light irradiation. These behaviors of the normalized two-photon fluorescence values in the single- and the multifocus excitations have clearly visualized the difference of the photo-induced cell damage progression, while were not obvious in the white-light transmission images (Figures 4(b) and 4(c)). These results indicated that the single-focus excitation induced greater damage compared with the multifocus excitation, and the damage might facilitate the uptake of DAPI molecules into cells and/or inhibit the excretion of DAPI molecules without any morphological changes.

We also performed the statistical evaluation of the temporal progression of the photo-induced cell damage as shown in Figure 5. We examined the temporal behavior of the normalized two-photon fluorescence value $S_{damage,TPF}$ of 12 cells for the single-focus excitation, 8 cells for the multifocus excitation and 4 cells for the control condition. Averaged normalized two-photon fluorescence values $S_{damage,TPF}$ of the single- and the multifocus excitations and the control condition were shown in Figure 5(a). The averaged normalized two-photon fluorescence values of the single-focus excitation at 20 min reached to 3.0 times greater than that of the multifocus excitation. This difference might indicate the difference of the degree of the photo-induced cell damage between the single- and the multifocus excitations. The standard deviation of the single-focus excitation also increased depending on the laser irradiation time, indicating the degree of the photo-induced cell damage relatively varied among the cells.

The statistical analysis using Student's t-test was also performed. For the comparison between the single-focus excitation and the control condition (Figure 5(b)), the p value of the Student's t-test was beginning to fall at around 8 min after starting of the laser irradiation. Eventually, we obtained the significant difference ($p < 0.01$) at 16.4 min after starting of the laser irradiation. In contrast, for the comparison between the multifocus excitation and the control condition (Figure 5(c)), significant difference was not obtained within 20 min after starting of the laser irradiation. For the comparison between the single- and the multifocus excitations (Figure 5(d)), the p value of the Student's t-test was beginning to fall at around 5 min, and the significant difference ($p < 0.01$) was obtained at 17.2 min after starting the laser irradiation, which was almost identical to the result of the comparison between the single-focus excitation and the control condition. These results indicated that the multifocus excitation apparently reduced photo-induced cell damage compared with the single-focus excitation in the condition to obtain the same CARS signal.

We also confirmed the temporal behavior of the photo-induced cell damage with a one-photon fluorescence scheme. The one-photon fluorescence scheme employed an ultraviolet light source for the observation of one-photon fluorescence of DAPI fluorophores, while picosecond pulsed laser with the single- or multifocus excitation scheme was used as a laser source for the cell damage induction. High signal-to-noise ratio observation of DAPI fluorophores would be expected in the one-photon fluorescence scheme owing to the high excitation efficiency via the one-photon process. One-photon fluorescence observation of DAPI and the near-infrared light irradiation with the single- or multifocus excitation scheme were performed sequentially. The one-photon fluorescence was observed every 2 min with the exposure time of 1 s, while the near-infrared light irradiation with the single- or multifocus excitation scheme was performed on the other time. We normalized the one-photon fluorescence intensity of DAPI as follows:

$$S_{damage,OPF} = \frac{I_{OPF}}{I_{ex}}, \tag{4}$$

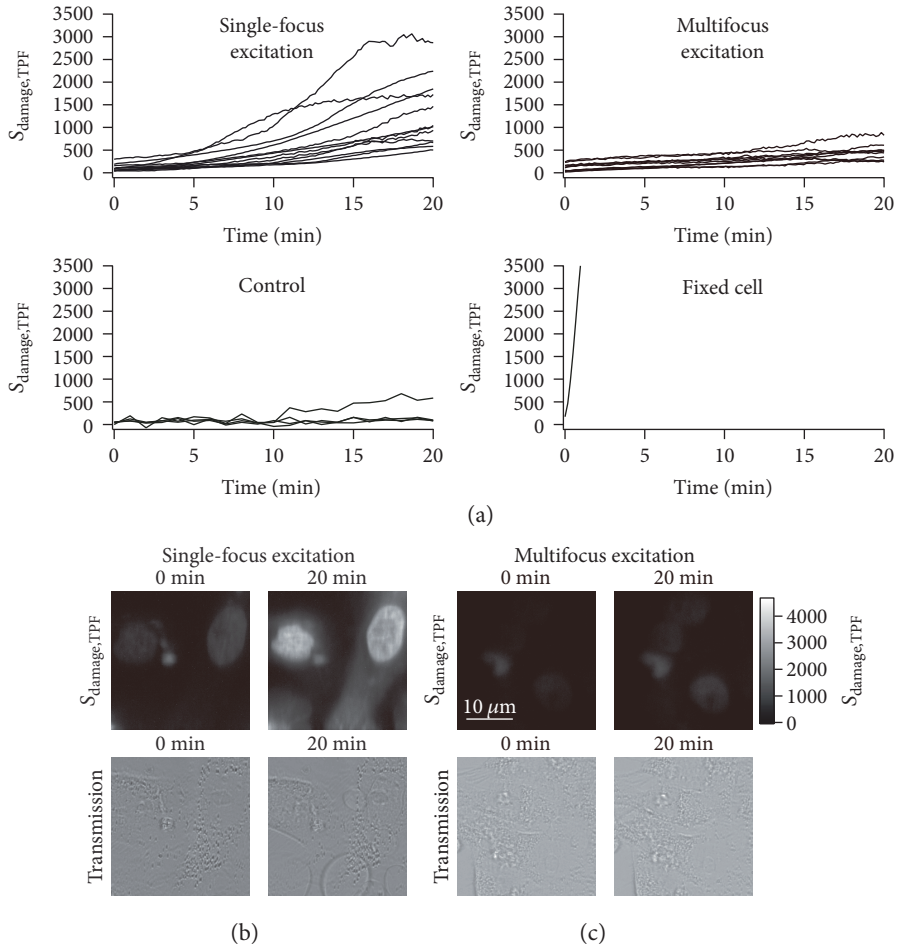

Figure 4: Temporal behaviors of the normalized two-photon fluorescence values $S_{damage,TPF}$ observed at the nucleus of HeLa cells. (a) Temporal behaviors of the normalized two-photon fluorescence values of the nucleus of individual cells with the single-focus excitation, the multifocus excitation, the control condition, and the fixed HeLa cell condition. Typical normalized two-photon fluorescence and white-light transmission images after starting of the laser irradiation of 0 and 20 min with (b) the single- and the (c) the multifocus excitations.

where $S_{damage,OPF}$, I_{OPF}, and I_{ex} are the normalized one-photon fluorescence signal for photo-induced cell damage analysis, the one-photon fluorescence signal observed with an image sensor and the excitation laser power, respectively. Since the optical setup of the one-photon fluorescence obseritations and the control condition, the effect of the one-photon fluorescence observation on the evaluation of the photo-induced cell damage was identical in these conditions.

The normalized one-photon fluorescence values $S_{damage,OPF}$ of the single- and multifocus excitations, and the control condition are shown in Figure 6. As similar to the results of the two-photon fluorescence evaluation of the photo-induced cell damage, the normalized one-photon fluorescence values $S_{damage,OPF}$ of the single-focus excitation significantly increased rather than the multifocus excitation (Figures 6(a) and 6(b)). However, in the condition of the irradiation laser power of 27.8 mW for the single-focus excitation and 14.5 mW with 7 focal spots for the multifocus excitation, which was the same condition of Figures 4 and 5, the normalized one-photon fluorescence values increased relatively faster than those evaluated with the two-photon fluorescence scheme (Figure 6(c)). This might be because of the additional effect of ultraviolet light irradiation, which was performed for the excitation of one-photon fluorescence of DAPI fluorophores. This effect was clearly observed in the control condition (Figure 6(c)), in which the near-infrared irradiation was not performed. Furthermore, at around 25 min after starting the near-infrared laser irradiation, the normalized one-photon fluorescence value of the single-focus excitation was beginning to fall. This might be because of the photobleaching of the DAPI fluorophores at the nucleus of HeLa cells. Although these unfavorable effects due to the ultraviolet light irradiation appeared, the lower photo-induced cell damage on the multifocus excitation than that on the single-focus excitation was also demonstrated with the one-photon fluorescence scheme by the observation of the temporal behaviors of the normalized one-photon fluorescence values.

We also compared low and high laser power irradiation conditions for the single- and multifocus excitation. For the high laser power condition, the irradiation laser power of each spot (I_{ex}) was set at 27.8 mW and 14.5 mW for the single- and the multifocus (7 focal spots) excitations, respectively. In contrast, the irradiation laser power of each spot

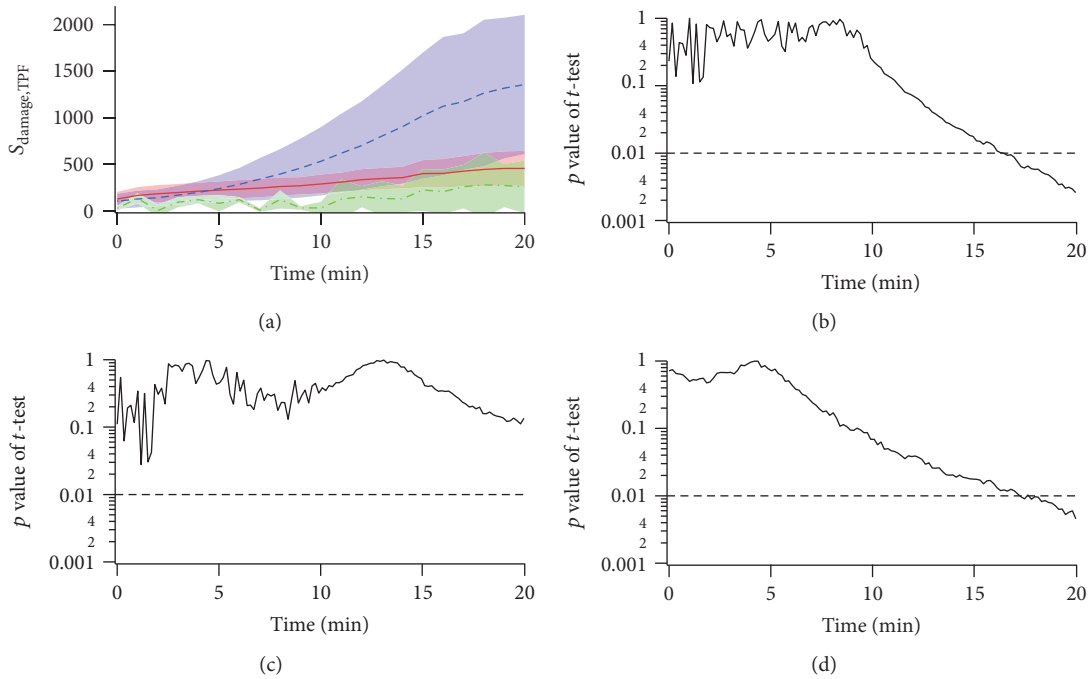

FIGURE 5: Statistical analysis of the temporal behavior of the normalized two-photon fluorescence value $S_{damage,TPF}$ observed at the nucleus of HeLa cells. (a) Averaged temporal behaviors of the normalized two-photon fluorescence values of the nucleus of HeLa cells with the single-focus excitation (blue dashed line), the multifocus excitation (red solid line), and the control condition (green one-dotted chain line). Shaded area indicates standard deviation. p value of Student's t-test comparing (b) the single-focus excitation and the control condition, (c) the multifocus excitation and the control condition, and (d) the single- and the multifocus excitations.

(I_{ex}) was, respectively, set at 13.3 mW and 7.0 mW for the single- and the multifocus (7 focal spots) excitations for the low laser power condition. In the high laser power irradiation condition, we obtained the significant difference ($p < 0.01$) at 2.0 min, 9.6 min, and 5.9 min after starting of the laser irradiation for the comparison between the single-focus excitation and the control condition, the multifocus excitation and the control condition, and the single- and the multifocus excitations, respectively. Meanwhile, the significant difference was not obtained in the low laser power irradiation condition within 40 min after starting of the laser irradiation even though the same total energy of the laser irradiation of the high laser power irradiation condition was reached with about twice of the exposure time in the low laser power irradiation condition. This result suggested that the multifocus excitation scheme was more effective for the reduction of photo-induced damage as the laser irradiation power became higher.

4. Discussion

Our recent study proposed a multifocus excitation scheme for CARS microscopy for high-speed molecular imaging [9]. Here, we confirmed the efficacy of the multifocus excitation CARS microscopy in terms of cell viability by utilizing DAPI fluorophores. We found a lower uptake of DAPI fluorophores into HeLa cells during the multifocus excitation compared with the single-focus excitation scheme, indicating the reduction of photo-induced cell damage in the multifocus excitation. Our findings suggested that the multifocus excitation scheme is expected to be suitable for high-speed CARS microscopy in terms of minimal invasiveness.

A multifocus excitation scheme has been applied to one- and multiphoton microscopies [9, 17–23]. Especially in fluorescence microscopy, photo-induced damage has been well characterized. In the fluorescence microscopy, the photo-induced cell damage is predominantly caused via fluorescent dyes due to thermal stress, oxidation stress, free-radical generation, and so on. In contrast, since near-infrared picosecond pulsed lasers are employed and no dye is required, the photo-induced cell damage in the CARS microscopy is predominantly caused via the light absorption by the cell itself. Therefore, the mechanism of photo-induced damage in the multifocus CARS microscopy might be different from the multifocus fluorescence microscopy.

The photo-induced damage of CARS microscopy might be caused via multiphoton process rather than via one-photon process because of the low one-photon absorption of cells in the near-infrared region. The multiphoton process possibly induces thermal stress, oxidation stress, free-radical generation, and so on. For example, the photo-induced productions of DNA such as pyrimidine dimers and pyrimidine pyrimidone photoproducts can be initiated via the absorption of ultraviolet light at C = C double bonds in DNA that corresponds to the three-photon absorption of the near-infrared light [25–28]. Reactive oxygen species such as singlet oxygen ($^1O_2$) can be generated by the energy transfer from the excited chromophores in cells, such as flavin and porphyrin, via two- or three-photon absorption of near-infrared

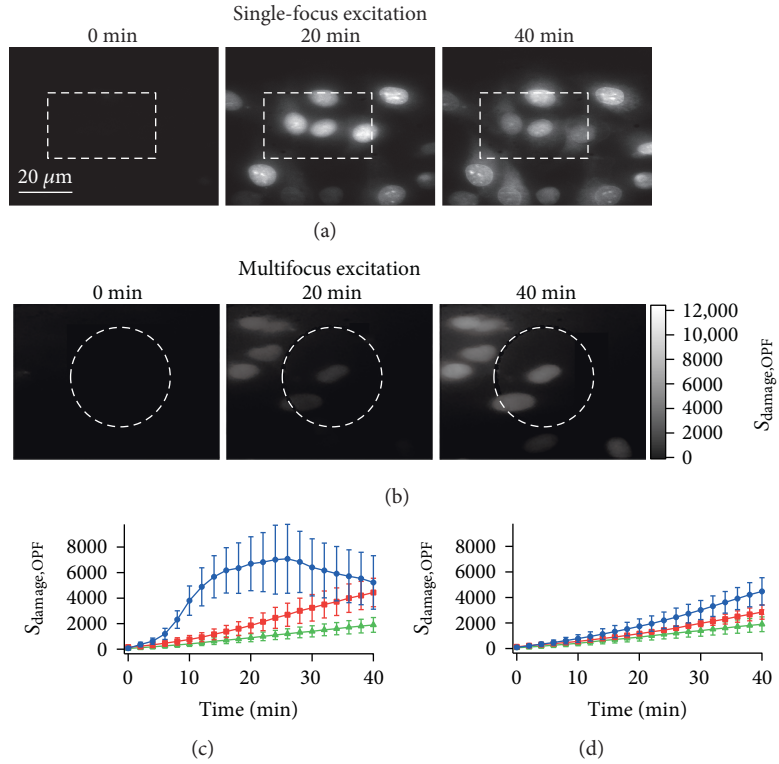

Figure 6: One-photon florescence analysis of photo-induced cell damage with DAPI fluorophores. Typical normalized one-photon fluorescence images after starting of the laser irradiation of 0, 20, and 40 min with (a) the single- and (b) the multifocus excitations. Dashed squares and dashed circles indicate the region of near-infrared light irradiation for the cell damage induction. Temporal behavior of one-photon fluorescence of DAPI fluorophores at the cell nucleus with (c) high and (d) low laser power irradiation conditions under the single-focus excitation (blue circle), the multifocus excitation (red square), and the control condition (green triangle). Error bars indicate standard deviation.

light to oxygen molecules near the chromophores [29–31]. The reactive oxygen species easily react with surrounding molecules and cause an oxidative damage to proteins, DNAs, and lipids. The probability of the multiphoton events increases nonlinearly proportional to the peak power of an excitation laser, indicating the peak power of the excitation laser supposedly plays an important role of photo-induced cell damage in CARS microscopy rather than the mean power of the excitation laser. As our results show, the multifocus excitation scheme significantly reduced photo-induced damage owing to the parallel arrangement of focal spots instead of the increase of focal laser power to obtain a sufficient CARS signal.

5. Conclusion

In the present study, we investigated photo-induced damage on living cells during single- and multifocus excitations for CARS microscopy. By utilizing DAPI fluorophores, we revealed the advantage of the multifocus excitation scheme in terms of cell viability. Although further studies such as the dependency of sample species, pulse duration, and the number of focal spots with a large number of samples are required for the detailed characterization of the photo-induced damage in the multifocus excitation scheme, our results suggest that the CARS microscopy with the multifocus excitation scheme will be a key solution for high-speed molecular imaging while minimizing photo-induced damage.

Conflicts of Interest

The authors declare that they have no conflicts of interest.

Acknowledgments

The authors thank Ms. N. Takeichi and Ms. S. Lewis, Tokushima University, for the English proofreading of the manuscript. This work was partially supported by the Grant-in-Aid for Scientific Research from the Ministry of Education, Culture, Sports, Science and Technology (MEXT) and the Development of Systems and Technology for Advanced Measurement and Analysis (SENTAN) program from the Japan Science and Technology Agency (JST). One of the authors (Takeo Minamikawa) acknowledges support by the Grant-in-Aid for JSPS Fellows from the Japan Society for the Promotion of Science (JSPS).

References

[1] A. Zumbusch, G. R. Holtom, and X. S. Xie, "Three-dimensional vibrational imaging by coherent anti-Stokes Raman

scattering," *Physical Review Letters*, vol. 82, no. 20, pp. 4142–4145, 1999.

[2] M. Hashimoto and T. Araki, "Coherent anti-Stokes Raman scattering microscope," *Proceedings of SPIE*, vol. 3749, pp. 496-497, 1999.

[3] H. Kano and H. Hamaguchi, "Femtosecond coherent anti-Stokes Raman scattering spectroscopy using supercontinuum generated from a photonic crystal fiber," *Applied Physics Letters*, vol. 85, pp. 4298–4300, 2004.

[4] X. S. Xie, J. Yu, and W. Y. Yang, "Living cells as test tubes," *Science*, vol. 312, pp. 228–230, 2006.

[5] C. W. Freudiger, W. Min, G. R. Holtom, B. Xu, M. Dantus, and X. Sunney Xie, "Highly specific label-free molecular imaging with spectrally tailored excitation-stimulated Raman scattering (STE-SRS) microscopy," *Nature Photonics*, vol. 5, pp. 103–109, 2011.

[6] Y. Ozeki, W. Umemura, Y. Otsuka et al., "High-speed molecular spectral imaging of tissue with stimulated Raman scattering," *Nature Photonics*, vol. 6, pp. 844–850, 2012.

[7] D. X. Lioe, K. Mars, S. Kawahito et al., "A stimulated Raman scattering CMOS pixel using a high-speed charge modulator and lock-in amplifier," *Sensors*, vol. 16, no. 4, p. 532, 2016.

[8] C. L. Evans, E. O. Potma, M. Puoris'haag, D. Cote, C. P. Lin, and X. S. Xie, "Chemical imaging of tissue in vivo with video-rate coherent anti-Stokes Raman scattering microscopy," *Proceedings of the National Academy of Sciences of the United States of America*, vol. 102, no. 46, pp. 16807–16812, 2005.

[9] T. Minamikawa, M. Hashimoto, K. Fujita, S. Kawata, and T. Araki, "Multi-focus excitation coherent anti-Stokes Raman scattering (CARS) microscopy and its applications for real-time imaging," *Optics Express*, vol. 17, no. 12, pp. 9526–9536, 2009.

[10] F. P. Henry, D. Cote, M. A. Randolph et al., "Real-time in vivo assessment of the nerve microenvironment with coherent anti-Stokes Raman scattering microscopy," *Plastic and Reconstructive Surgery*, vol. 123, Supplement 2, pp. 123S–130S, 2009.

[11] K. Konig, H. Liang, M. W. Berns, and B. J. Tromberg, "Cell damage in near-infrared multimode optical traps as a result of multiphoton absorption," *Optics Letters*, vol. 21, no. 14, pp. 1090–1092, 1996.

[12] K. Konig, T. W. Becker, P. Fischer, I. Riemann, and K. J. Halbhuber, "Pulse-length dependence of cellular response to intense near-infrared laser pulses in multiphoton microscopes," *Optics Letters*, vol. 24, no. 2, pp. 113–115, 1999.

[13] A. Hopt and E. Neher, "Highly nonlinear photodamage in two-photon fluorescence microscopy," *Biophysical Journal*, vol. 80, no. 4, pp. 2029–2036, 2001.

[14] Y. Fu, H. Wang, R. Shi, and J. X. Cheng, "Characterization of photodamage in coherent anti-Stokes Raman scattering microscopy," *Optics Express*, vol. 14, no. 9, pp. 3942–3951, 2006.

[15] T. Minamikawa, H. Niioka, T. Araki, and M. Hashimoto, "Real-time imaging of laser-induced membrane disruption of a living cell observed with multifocus coherent anti-Stokes Raman scattering microscopy," *Journal of Biomedical Optics*, vol. 16, no. 2, article 021111, 2011.

[16] H. Cahyadi, J. Iwatsuka, T. Minamikawa, H. Niioka, T. Araki, and M. Hashimoto, "Fast spectral coherent anti-Stokes Raman scattering microscopy with high-speed tunable picosecond laser," *Journal of Biomedical Optics*, vol. 18, no. 9, article 096009, 2013.

[17] E. Wang, C. M. Babbey, and K. W. Dunn, "Performance comparison between the high-speed Yokogawa spinning disc confocal system and single-point scanning confocal systems," *Journal of Microscopy*, vol. 218, Part A, pp. 148–159, 2005.

[18] J. Y. Tinevez, J. Dragavon, L. Baba-Aissa et al., "A quantitative method for measuring phototoxicity of a live cell imaging microscope," *Methods in Enzymology*, vol. 506, pp. 291–309, 2012.

[19] P. J. Ross, G. I. Perez, T. Ko, M. S. Yoo, and J. B. Cibelli, "Full developmental potential of mammalian preimplantation embryos is maintained after imaging using a spinning-disk confocal microscope," *BioTechniques*, vol. 41, no. 6, pp. 741–750, 2006.

[20] K. Yamagata, R. Suetsugu, and T. Wakayama, "Long-term, six-dimensional live-cell imaging for the mouse preimplantation embryo that does not affect full-term development," *The Journal of Reproduction and Development*, vol. 55, no. 3, pp. 343–350, 2009.

[21] J. Bewersdorf, R. Pick, and S. W. Hell, "Multifocal multiphoton microscopy," *Optics Letters*, vol. 23, pp. 655–657, 1998.

[22] J. Qu, L. Liu, Y. Shao, H. Niu, and B. Z. Gao, "Recent progress in multifocal multiphoton microscopy," *Journal of Innovative Optical Health Sciences*, vol. 5, no. 3, article 1250018, 2012.

[23] M. Kobayashi, K. Fujita, T. Kaneko, T. Takamatsu, O. Nakamura, and S. Kawata, "Second-harmonic-generation microscope with a microlens array scanner," *Optics Letters*, vol. 27, no. 5, pp. 1324–1326, 2002.

[24] T. Minamikawa, Y. Murakami, N. Matsumura et al., "Photo-induced cell damage analysis for multi-focus CARS microscopy," *Proceedings of SPIE*, vol. 7903, article 79032H, 2011.

[25] R. B. Setlow and W. L. Carrier, "Pyrimidine dimers in ultraviolet-irradiated DNA's," *Journal of Molecular Biology*, vol. 17, pp. 237–254, 1966.

[26] R. A. Meldrum, S. W. Botchway, C. W. Wharton, and G. J. Hirst, "Nanoscale spatial induction of ultraviolet photoproducts in cellular DNA by three-photon near-infrared absorption," *EMBO Reports*, vol. 4, no. 12, pp. 1144–1149, 2003.

[27] F. Fischer, B. Volkiner, S. Puschmann et al., "Assessing the risk of skin damage due to femtosecond laser irradiation," *Journal of Biophotonics*, vol. 1, no. 6, pp. 470–477, 2008.

[28] D. Trautlein, M. Deibler, A. Leitenstorfer, and E. Ferrando-May, "Specific local induction of DNA strand breaks by infrared multi-photon absorption," *Nucleic Acids Research*, vol. 38, no. 3, article e14, 2010.

[29] J. L. Ravanat, P. Di Mascio, G. R. Martinez, M. H. G. Medeiros, and J. Cadet, "Singlet oxygen induces oxidation of cellular DNA," *The Journal of Biological Chemistry*, vol. 275, no. 51, pp. 40601–40604, 2000.

[30] C. Kielbassa, L. Roza, and B. Epe, "Wavelength dependence of oxidative DNA damage induced by UV and visible light," *Carcinogenesis*, vol. 18, no. 4, pp. 811–816, 1997.

[31] J. Cadet, M. Berger, T. Douki et al., "Effects of UV and visible radiation on DNA - final base damage," *Biological Chemistry*, vol. 378, no. 11, pp. 1275–1286, 1997.